Resonant SRS Filtering Fiber for High Power Fiber Laser Applications

Christophe A. Codemard, Natasha T. Vukovic, Jaclyn S. Chan, Paulo J. Almeida, John R. Hayes, Marco N. Petrovich, Catherine Baskiotis, Andy Malinowski, and Michalis N. Zervas

***Abstract*—We explore the properties of a novel stimulated Raman scattering (SRS) filtering fiber for high average or high peak optical power delivery applications. The fiber geometry is based on a series of circularly arranged high index rods embedded in a leaky silica cladding. The operation principle relies on the resonant coupling of the core and rod modes and the wavelength dependent leaking of the structure. The fabricated fiber demonstrated wide transmission window and filtering of SRS with extinction in excess of 20dB at the Raman Stokes wavelength, excellent robustness with bending, and high output beam quality. The fiber has been tested as a beam delivery fiber of a commercial pulsed fiber laser system in order to explore the filtering performance and its limitations.**

***Index Terms*— Stimulated Raman Scattering, High Power Fiber Laser, Beam delivery.**

I. Introduction

FIBER lasers have grown to become mainstream industrial photon engines and have expanded into many sectors of the materials processing industry, thanks to their superior performance, including high-power superior beam quality and stability, high brightness, as well as efficient thermal management and minimization of thermal effects [1]. The progress of this latest high power laser technology is largely due to the outstanding characteristics of fibers as an active medium. However, the increase of optical power and tight guidance leads inevitably to some unwanted nonlinear effects, such as self-focusing, self-phase modulation, stimulated Brillouin scattering (SBS), and stimulated Raman scattering (SRS) [1],[2]. Although the ultimate limit on the laser performance is set by self-focusing, it is considered that self-phase modulation is a limiting effect for short pulses (<0.5ns), SBS is detrimental effect for narrow linewidth, long pulses (>2ns), while SRS is a limiting nonlinearity for spectral broadband signals in any temporal regime [2], [3]. SRS is a stimulated process leading to efficient Raman amplification. At high optical power density, SRS leads to scattering and energy transfer from the optical signal into the first Stokes, and then in a cascaded fashion to second and higher order Stokes [4]. This limits the available output power in fiber lasers at a given signal wavelength. Because SRS is a nearly instantaneous process, it is considered the main obstacle for power scaling of broadband pulsed fiber systems, and in particular when single-mode core fibers (V<2.4) are employed, in which case the SRS threshold is significantly reduced [5]. In the continuous wave (CW) regime, in addition to transverse mode instability and pump brightness, SRS is considered to be the most limiting nonlinear effect of practical multi-kW class high power fiber lasers with beam delivery [6]. Therefore, there is a need to overcome or push the limits at higher optical powers, and in particular suppression of SRS remains an important challenge.

To date, a number of various techniques and designs have been considered for the suppression of detrimental SRS, such as employing long-period gratings to attenuate the scattered beam [7]. Moreover, there were attempts to suppress SRS using special fibers, including resonant rings design [8]-[11], and photonic bandgap fibers [12]-[15]. However, in those designs, despite the Raman filtering due to the resonant coupling between core and cladding modes, the fiber bending must be carefully controlled, or only short fiber lengths are permitted. SRS suppression has also been demonstrated based on wavelength dependent bending loss [16],[17], but this approach suffers from significant amount of loss at the signal wavelength too.

In this paper we first present the performance of a W-type fiber with high index concentric rings imbedded in the depressed index region (design#1), and its effectiveness in the suppression of SRS. The experimental characterization showed that design#1 suffers from undesired coupling of core to high-order ring modes, which reduce dramatically the transmission window and increase the tolerance in the fiber's structural parameters, even in the case of unbent fiber. In order to improve the fiber SRS filtering performance, we employed a different strategy (design#2) [18], and demonstrated a novel fiber design for the efficient suppression of SRS, under straight and bent conditions. The fiber structure is based again on a W-type fiber with the high index concentric rings replaced with high index rods. In this case, the series of circularly arranged rods breaks the azimuthal symmetry of the concentric rings, so that no individual rod mode crosses the dispersion curve of the fundamental core mode near the designed operating wavelength. The basic mechanism relies on the effective refractive index matching and resonant

N. T. Vukovic, J. S. Chan, M. N. Petrovich, J. R. Hayes, and M. N. Zervas are (and C. Baskiotis was) with the Optoelectronics Research Center of the University of Southampton, Southampton, SO17 1BJ, United Kingdom (e-mail: ntv@orc.soton.ac.uk);J.S.Chan@soton.ac.uk;mnp@orc.soton.ac.uk; m.n.zervas@soton.ac.uk).

C. A. Codemard, P. Almeida, and A. Malinowski are with the SPI Lasers UK Ltd, Southampton, SO30 2QU, United Kingdom (email: Christophe.Codemard@spilasers.com; paulo.almeida@spilasers.com; Andy.Malinowski@spilasers.com;).

The work was supported in part by the Royal Academy of Engineering under the Research Chairs and Senior Research Fellowships scheme.

coupling between core and cladding modes supported by the rod structure. We show that this fiber has advantages in comparison to the resonant ring designs and that it is suitable for applications of high power pulsed laser beam delivery applications.

II. SRS FILTERING FIBER DESIGNS

In this paper we first investigate the potential of SRS filtering fibers with cylindrical symmetry for high power delivery applications. In particular, the specifications included: negligible bend loss at 10cm radius, negligible fundamental mode loss (less than 0.01dB/m) at the signal wavelength, greater than 100dB total loss at the Raman wavelength for the SRS suppression in high average (kW level) or high peak (>200kW) optical power delivery applications. Inspired by a work on active cladding pumped step index fibers [9], we started our investigation with the passive W-type fiber with the addition of one or two high refractive index concentric rings in the inner cladding. Then we extended this study into W-type fibers with added high index dielectric rods in the cladding.

A. W-type Fibers with Imbedded Concentric Rings – Design#1

We started our study with the W shaped fiber with the depressed cladding, and extended it to the addition of one or two added rings. The main advantage of W-type fibers with added rings, as compared to e.g. step index fibers previously reported in the literature [8, 9], rest in the fact that, in addition to the field delocalization, a higher level of Raman suppression can be achieved with respect to W-shape profile, even in the unbent fiber.

The refractive index profile and principle of operation of W-type fiber with two imbedded high index rings is shown schematically in Fig. 1. The step index fiber, surrounded by two rings, placed optimally in the depressed inner fiber cladding (delocalization area), has been engineered to ensure resonant coupling from the fundamental core mode to ring modes at Raman wavelengths. The depressed inner cladding is surrounded by a raised-index outer cladding (loss area) which provides leakage loss to the outer ring modes.

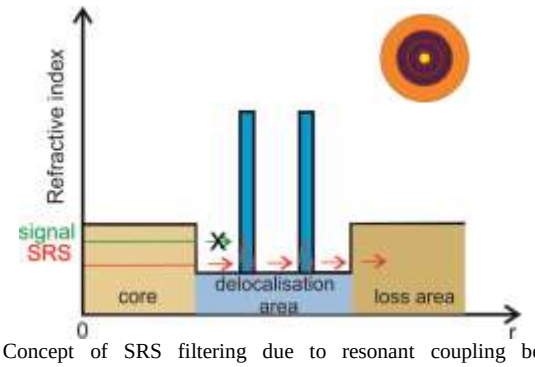

Fig. 1. Concept of SRS filtering due to resonant coupling between fundamental core and high order cladding modes (design#1); no coupling occurs at signal wavelength. Inset: cross section of a W-type fiber with high index rings.

In order to introduce substantial differential loss between the desired signal and parasitic SRS wavelengths, the proposed fiber design combines wavelength-dependent mode delocalization and spatially dependent loss mechanisms. The mode delocalization is achieved through multi-stage resonant coupling between the fundamental core mode and the appropriately designed high-index ring modes. At the resonant Raman wavelength, where the effective index of the core and concentric rings are matched, the fiber fundamental mode becomes highly delocalized and spreads-out in the cladding through successive couplings in the high index rings and the leaky outer cladding modes. In contrast, at the signal wavelength the fundamental mode is not phase matched with the surrounding rings and remains highly localized in the core.

To better understand the guidance properties of this fiber we used a full vector modal solver based on Finite Element Method (implementation based on COMSOL Multiphysics). Due to the presence of the raised-index outer cladding (loss area) all supported modes are in principle and to varying degrees leaky and therefore characterized by complex propagation constants. Figure 2 plots the leakage loss (α) which is related to the imaginary part of the propagation constant (β) of the lowest-order (highest effective index) fiber mode, as a function of wavelength, calculated from the equation: $\alpha(dB/m) \approx 8.686\,\mathrm{Im}(\beta)$. It is shown that around and below the signal wavelength band (~1070nm) the leakage loss is low (<0.01dB/m) and the mode is localized in the core (see inset lower mode intensity profile). Around the 1st SRS Stokes wavelength (~1125nm) the leakage loss shows a maximum of ~100dB/m. In this case, the mode profile is highly delocalized and extending into the concentric rings (see inset upper field intensity profile), as a results of phase matching and strong coupling. However, in spite of a good filtering in the straight fiber and good bend performance for large bend radii, as well as the compatibility with modified chemical vapor deposition (MCVD) process, there are important drawbacks of this design. This includes unwanted coupling with numerous ring modes (marked with red arrows in Fig. 2), high fabrication tolerances of ±0.025 μm on high index ring thickness, and strong bend sensitivity. This shows as additional "spikes" in the leakage loss spectrum and it is more pronounced when the fiber is bent. Importantly, any imperfections, such as slight asymmetries, interface roughness between different layers, longitudinal non-uniformities, microbending etc., in the fabricated fiber lead to the additional resonant couplings/scattering from the fundamental mode to ring modes or between ring modes, as shown in Fig. 2.

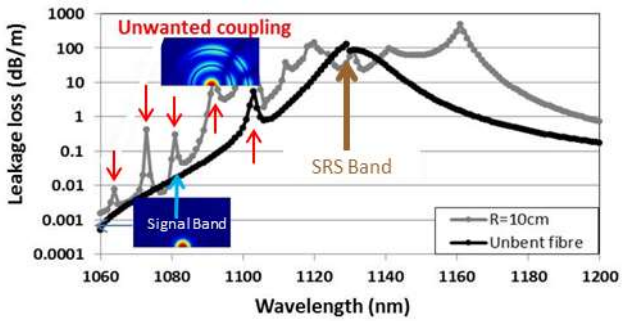

Fig. 2. Leakage spectrum of the fundamental core mode for the straight and coiled fiber (bending radius 10cm) (design#1). Red arrows indicate coupling to unwanted ring modes (one is shown in the top inset).

The fiber was fabricated using a standard MCVD process. Experiments were performed and showed complex loss spectra due to the presence of unwanted couplings and interaction with the multiple ring modes (as the theory in Fig. 2 predicts).

Also, we compared the impact of added rings in the cladding, and results are shown in Fig. 3. We identified and optimized fiber parameters of the W shaped fiber to match the stringent requirements on mode field diameter, bend loss, and single modality.

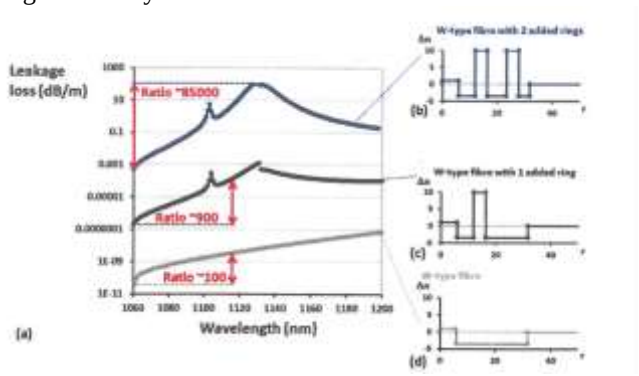

Fig. 3. (a) Leakage loss spectrum of the fundamental core mode of a W-type fiber without added ring (gray) and with one (black) and two (blue) ring(s) in the cladding. (b) Refractive index profile of the W-type fiber with two added rings, (c) Refractive index profile of the W-type fiber with one added ring. (d) Refractive index profile of the W-type fiber without added ring.

Results in Fig. 3 reveal that it would be completely unfeasible to obtain the high level of SRS rejection while meeting all three other specifications in a conventional W shaped fiber structure. However, the addition of ring of suitable geometry and index profile allows increasing the ratio between the leakage loss of the fundamental mode at the Raman wavelength and the signal wavelength by a factor of ~9. At the same time, the leakage loss of the fundamental mode at all wavelengths is increased by more than three orders of magnitude (and therefore not suitable for practical implementation). On the other hand, the addition of two additional rings would allow increasing the Raman/signal wavelength rejection by a factor >850. Based on the results in Fig. 2 and Fig. 3, we concluded that modified W-type fiber design with the addition of resonant rings can produce fiber designs which theoretically satisfy most of the target requirements. However, the unwanted couplings from the core mode to the high order azimuthal ring modes, as observed in fabricated fibers (Fig. 2), and high sensitivity seriously limit their practical implementation. Therefore, there is a need to look for a design which allows larger fabrication tolerances, while ensuring large higher order mode suppression and presenting a lower number of ring modes with a dispersion curve intersecting that of the fundamental mode near the operating wavelength.

B. W-type Fiber with Imbedded High Index Dielectric Rods - Design#2

Due to the experimental observation of a large number of azimuthal modes present near the signal wavelength band in design#1, here we propose a new fiber design, which incorporates circularly arranged individual high index rods in the fiber's depressed inner cladding instead. The advantage of this approach is that since the series of circularly arranged rods break the inherent azimuthal symmetry of resonant rings, no rod-mode crosses the dispersion curve of the fundamental mode near the designed operating wavelength, and previously occurring unwanted couplings between the core mode and numerous ring modes are prevented. As in design#1, the operating principle of this fiber relies on the wavelength dependent power delocalization through the multi-stage resonant coupling between the core mode and the appropriately designed high-index rods placed optimally in the composite fiber depressed inner cladding (delocalization area), as shown in Fig. 4. Again, the raised index outer cladding (loss area) provides sufficient leakage loss for the adjacent outer rods.

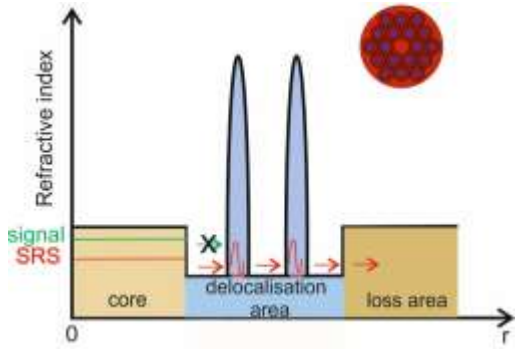

Fig. 4. Refractive index distribution schematic in a W-type fiber with incorporated parabolic profile high index rods (design#2). Inset: fiber cross section.

III. SRS FILTERING FIBER WITH HIGH INDEX RODS MODELLING

The proposed SRS mitigating fiber structure (design#2) comprises standard silica core and Germanium (Ge)-doped high index rods embedded in fluorine (F)-doped tubes in a hexagonal lattice in the pure silica outer leaky layer, as shown in Fig. 5(a). The refractive index profile of the structure is given in Fig. 5(b). The important structural parameters that define the fiber are the silica core diameter 15μm, and the ratio of fluorinated cladding diameter (D_F) and Ge-rod core diameter (D_{Ge}) is ~2.394. Importantly, the refractive index profile of Ge-rods is measured (using an Intertronics Fiber Analyzer (IFA)) and interpolated, giving the parabolic profile raised index of Δn_{Ge} = 2%. The refractive index difference of a depressed fluorinated cladding is Δn_{core} = -0.15%. The fiber estimated core NA is ~0.07.

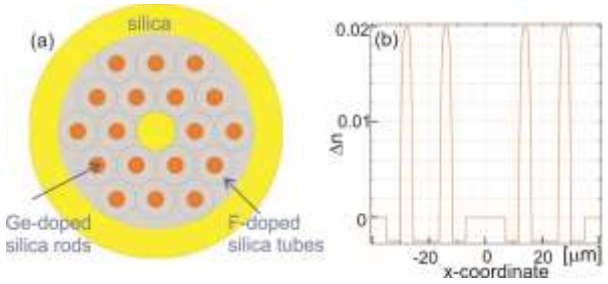

Fig. 5. (a) Cross section of a SRS filtering fiber design#2. (b) Line profile of a refractive index including parabolic graded-index inclusions.

The full vector finite element method modelling was performed to design the fiber and investigate its properties. The extensive modelling focused on fulfilling the rigorous specification, which includes SRS filtering efficiency, overall loss, bend loss, fiber modality, and mode field diameter, taking into account the measured refractive index of Ge rods. The model considered the actual refractive index distribution of the Ge-doped rods within the fiber cladding.

The numerical modelling was used to identify the parameters that enable phase-matching between the core mode and high order rod modes at Raman wavelength, and consequently to enable efficient SRS filtering, whilst keeping the loss at signal wavelength low. Typically, by tuning the core/cladding index contrast, the core size and/or the cladding structure, it is possible to greatly modify the number of guided modes as well as their dispersion properties. The parameters which satisfy the phase matching condition between the core LP_{01} mode and high order Ge-rods modes include Ge-rod core diameter ~6.27μm and the fluorinated tube diameter is 15μm. This fixes the rod core-to-core distance to Λ=15μm (such that D_F/Λ=1). The dispersion curves in Fig. 6(a) are based on modelling of the two different single core structures; the first is comprised of the silica core and fluorinated silica cladding, and the second comprises parabolic fiber with Ge-doped silica core and fluorinated silica cladding. As shown in Fig. 6(a), these parameters ensure phase matching and therefore efficient coupling and delocalization of the fundamental core mode LP_{01} to the LP_{21} and LP_{02} rod modes at the 1st Raman Stokes wavelength (~1125nm). At the signal wavelength band (~1070nm), on the other hand, fiber core and high index rods remain phase mismatched and therefore no substantial coupling (and power delocalization) is expected. Fig. 6(b) plots again the leakage loss of the lowest order fiber mode. The highest loss is obtained at the design SRS band wavelength (~1125nm) as a result of strong mode coupling to rod LP_{02} mode (see inset mode intensity profile). The LP_{31} mode is phase matched at ~800nm, well outside the signal wavelength band. The fibre provides some degree of higher-order mode delocalisation and higher propagation losses for the LP11 core mode, due to larger overlap with the surrounding leaky rod structure. Although the designed fiber can support 2 guided modes, single mode excitation can be ensured with careful splice optimization.

Further sensitivity analysis proved the robustness of the design and no performance variations for bending down to 10cm bending radii, as shown in Fig. 6(b). The leakage loss spectra remain unaffected by bending radii down to 20cm. For smaller bend radii (~10cm) the peak of the loss spectrum broadens to longer wavelengths around the Raman peak, while it remains largely unaffected around the signal wavelength. Numerical modelling indicates an order of magnitude significant differential bend loss for the LP_{11} mode in the signal band.

It is shown that the design parameters result in ~0.01dB/m loss at the signal wavelength band and ~100dB/m leakage loss at the SRS wavelength.

Inevitably, fabrication difficulties will have an impact on tolerances, and thus it is important to perform a parameter sweep, and to determine what parameters have a more significant impact. The detailed analysis which included impact of various geometrical parameters was conducted. Importantly, the simulation results reveal no performance variations with ±200nm random shifts in the rod positions in the low index cladding. Furthermore, the modelling suggests that the geometrical parameters would need to be satisfied to within approximately ±10% tolerance to achieve the required performance. This is a major improvement compared to design#1, in which the width of the trench in a W-fibre must be controlled to 25nm.

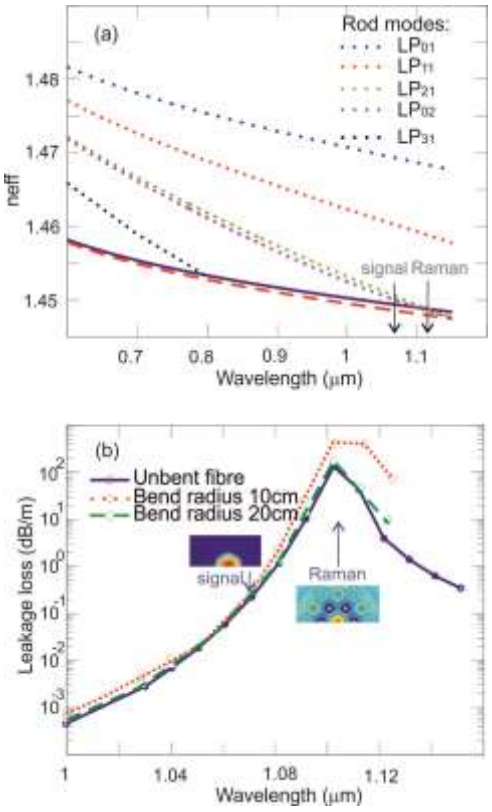

Fig. 6. SRS filtering fiber Design#2: (a) Effective indices of modes as a function of wavelength. Solid line corresponds to the LP_{01} (blue) and dashed line corresponds to LP_{11} (red) modes of the silica core modes; dotted lines correspond to the Ge-rod modes; (b) Effect of bend radius on a leakage loss of the SRS suppression fiber. The mode field diameter at 1070nm is ~17.5μm.

There is a trade-off between the high refractive index of the rods and the core size, the distance between the core and the rods, the number of rod layers and the desired SRS losses and fundamental mode propagation loss. The maximum refractive index availability from commercial Germanium doped rods and fabrication tolerance currently limits the maximum core design to about ~16μm for a SRS propagation of ~100dB/m. However, compromising on the SRS losses enable larger core and lower refractive index rods to be used.

IV. SRS FILTERING FIBER FABRICATION AND CHARACTERIZATION

In this section we report on the fabrication, transmission as well as bending loss characterization of the SRS filtering fiber with high index rods (design#2).

A. *Fiber Fabrication*

Fabricating optical fibers of complex structure with high Germanium content using stack and draw method poses in practice two interlinked fabrication challenges. These are related to getting the geometry right in the stack, and to dealing with materials with quite different properties. Important aspect is about ensuring tight tolerances on the homemade rods and tubes used in the stack and the risk of gaseous out-diffusion and bubble formation because of mixing different brought-in glasses. In particular, F-doped glass may or may not be in thermodynamic equilibrium, depending on how it was made [19]. Notably, we were not in control on the exact composition and how brought-in proprietary glass is made. Despite the fabrication challenges related to the relatively thin walls of the tubes, the fiber has been successfully fabricated using stack and draw method. Moreover, five different bands with slightly different dimensions were drawn, to satisfy the geometrical tolerances within ±4%. The microscopic image of a cross section of the SRS filtering fiber is shown in Fig. 7. It can be observed that nearly perfect hexagonal structure, and a good agreement with the design parameters, has been achieved.

Fig. 7. Microscope image of the SRS filtering fiber, scale = 20μm.

B. *Transmission Loss Characterization*

In order to characterize a fiber with respect to loss requirements, we used a broadband light source to launch light into the fiber. In our experiment, in order to minimize the excitation of the LP_{11} mode, we carefully launched light in the fundamental mode of the fiber. The fiber used in our experiments has outer diameter 260μm and core diameter 16μm. Fig. 8 shows transmission spectra for a 15cm long fiber. It can be observed that the fiber exhibits high loss of ~15dB in the designed Raman 1st Stokes wavelengths over a ~50nm bandwidth, whilst exhibiting low loss at the signal band wavelength (~1070nm). The high loss bands correspond to the intersection of the effective indices curves shown in Fig. 5(a). In addition to the Raman 1st Stokes loss band, which corresponds to efficient coupling to LP_{21} and LP_{02} rod modes, we observed a loss band just above 800nm, corresponding to coupling to LP_{31} rod modes. Notably, this result implies an excellent agreement between the prediction obtained from the numerical modelling and the experimental measurements, and it is also a justification of similarity between the real geometrical parameters of the drawn fiber and the original fiber design. In addition, we used a high resolution optical time domain reflectometer (OTDR), operating outside the filtering range at 1300nm, and measured a background loss of ~0.032dB/m, as shown in the inset of Fig. 8.

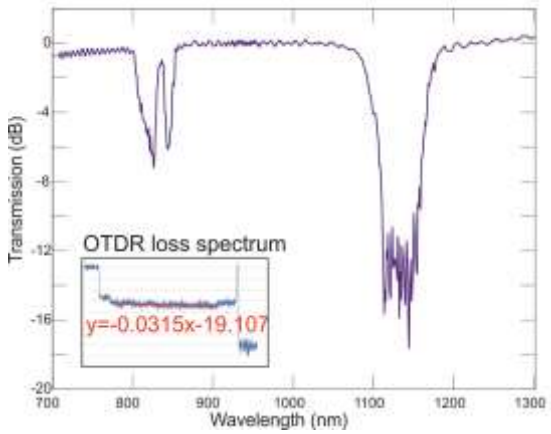

Fig. 8. Loss spectrum measurement for a 15cm long fiber. Inset: OTDR loss spectra, for ~9.5m long SRS suppression fiber (blue), and the corresponding linear fit (dashed red curve).

We also carried out a cut-back transmission measurement to establish the dependence of transmission on length. Fig. 9 shows transmission spectrum for two different lengths. The transmission spectrum shows two dips due to coupling into LP_{02} (shorter wavelength) and LP_{21} (longer wavelength) rod modes, as the design phase matching curves in Fig. 6(a) indicates. In addition, while the longer wavelength dip reduces, the shorter wavelength dip appears to be saturated and do not change with the length cut-back.

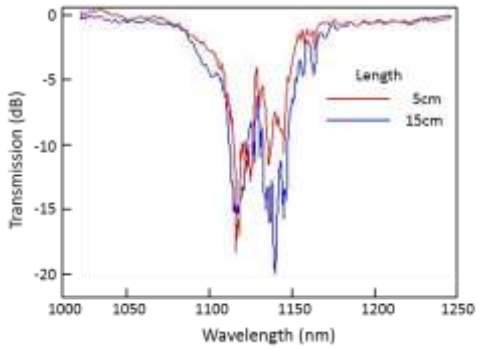

Fig. 9. Loss spectrum measurement for a 15cm and 5cm long fiber.

C. *Bending Loss Characterization*

In order to validate robustness to bending, as predicted by the modelling in Fig. 6(b), we used a broadband source and we bent the fiber with the small radius of 10cm and 6cm. The transmission spectra in Fig. 10 show very low sensitivity to bending. Most importantly and in sharp contrast with design#1 (c.f. Fig. 2), there is no unwanted coupling between the core mode and rod modes in the vicinity of signal wavelength when the fiber is bent. In the case of bent fiber, the loss spectrum, rather than shifting, expands to longer wavelengths, around the SRS band, while it remains largely unchanged around the signal band. This behavior is in very good agreement with the theoretical results in Fig. 6(b).

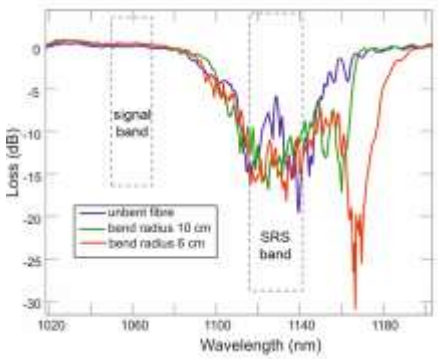

Fig. 10. Bending loss characterisation of a 15cm long fiber.

Fig. 10 shows that in addition to broadening the loss spectrum becomes stronger to longer wavelengths. This is believed to be due to bending-induced fundamental mode field shifting to the cladding, which results to stronger overlap with and coupling to rod modes.

V. VALIDATION OF RESULTS AND DISCUSSION

Propagation characteristics of SRS filtering fiber with high index rods were further analyzed using an in-house software based on beam propagation method (BPM).

The propagation of the electric field over 2m long SRS fiber with high index rods was calculated and the overall power as a function of wavelength and length is shown in Fig. 11. The results show two distinctive transmission dips in very good agreement with the experimental data shown in Fig. 9 and 10.

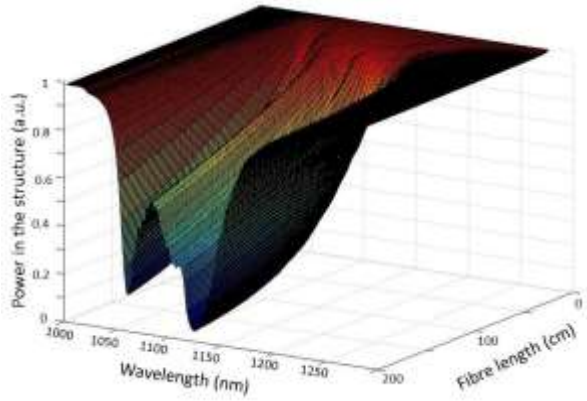

Fig. 11. Power spectrum evolution for a 2m long straight fiber.

Fig. 12 shows the power evolution along the length calculated at different wavelengths, including signal band wavelength and a range of wavelengths in Raman 1st Stokes band. It can be observed that the power does not follow linear dependence with fiber length. From the simulations and field plots associated with the wavelengths in Fig. 12, it can be concluded that the saturation of the power along the length is due to the high order rod modes being cross-coupled in the composite cladding and not leaking efficiently into the surrounding leaky layer. We anticipate that this is due to the different leakage loss associated with different high order modes of the composite rod arrangement. In spite of this property, it has been observed that even short length of this fiber (~5cm) could provide ~20dB SRS loss, which can be sufficient for many applications. This saturation behavior is in good agreement with the experimental results in Fig. 9.

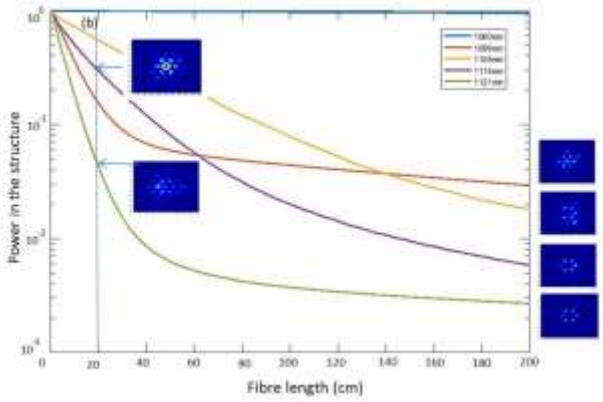

Fig. 12. Power as a function of length for a straight fiber at different wavelengths.

In addition, we modelled a 20cm long fiber with a bending diameter of 8cm, and the result is shown in Fig.13. The power evolution plot shows strong spectral broadening at the longer wavelength band, whilst keeping a sharp edge on the shorter wavelength side. This unique behaviour is associated with the formation of new super-modes obtained by coupling of high order rod modes due to bending. It is observed that the transmission loss spectrum broadens and becomes stronger at longer wavelengths, in very good agreement with the experimental results in Fig. 10.

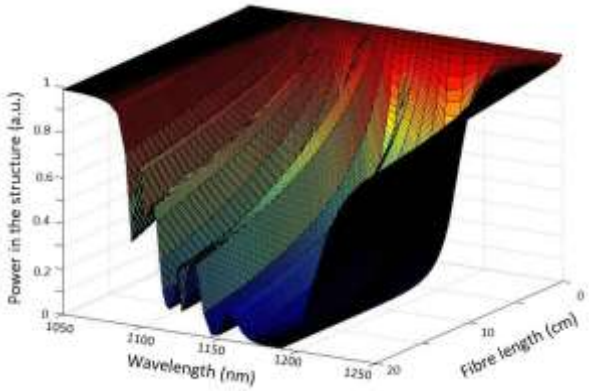

Fig. 13. Power spectrum evolution for 20cm long fiber with a bending diameter 8cm.

Fig. 14 shows power evolution calculated at different Raman Stokes wavelengths. Again, power saturation due to cross-coupling of modes and due to bending is observed.

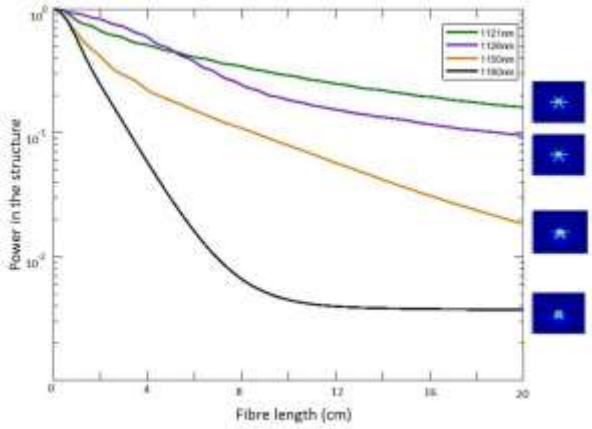

Fig. 14. Power as a function of length for a fiber with a bending diameter 8cm.

VI. SRS FILTERING FIBER LASER BEAM DELIVERY TESTING

The SRS fiber was tested as a beam delivery fiber of a commercial pulsed fiber laser operating at 1MHz with 2ns long pulses. The characterization setup is shown in Fig. 15. The light is launched to the SRS suppression fiber from a modified G4 fiber laser from SPI Lasers, which is capable of delivering 35kW peak power. The ~1m delivery fiber is spliced to the ~25cm of a step index fiber with the suitable mode field diameter, so that it can match the SRS suppression fiber. The SRS suppression fiber length was 9.5m, and it was coiled with 30cm and 15cm diameter. A short piece of the same step index fiber used at the input of the SRS was added at the end of the SRS fiber, with an additional 0.8mm end-cap, made of matched cladding size (250μm) coreless fiber.

Fig. 15. Experimental setup for the pulsed laser application.

The measurement results of the output spectra are shown in Fig. 16. The results clearly indicate that the SRS wavelength band is filtered out effectively from the output spectra, as no measurable emission is present above ~1100nm. In addition, the output beam M^2 was measured less than 1.1 (see inset of Fig. 16). Some astigmatism due to the angle-cleave on the end-cap can be also observed.

In Fig. 16, we observed that coiling only slightly impacted the transmitted signal peak power. However with the input power increase, the excess peak power that generates the SRS is filtered out as bending slightly modified the position of the spectral filtering edge. Furthermore, excess spectral broadening is observed with increased peak powers, which we attribute to enhanced four wave mixing (FWM) process in the SRS filtering fiber. Also, it can be noticed that the peak power is limited to ~3.5kW with a 9.5m long SRS suppression fiber, due to excess losses arising from FWM process, which ultimately sets the maximum peak power achievable. The average power in the experiments was in the range of ~4W (depending on pulse duration and repetition rate).

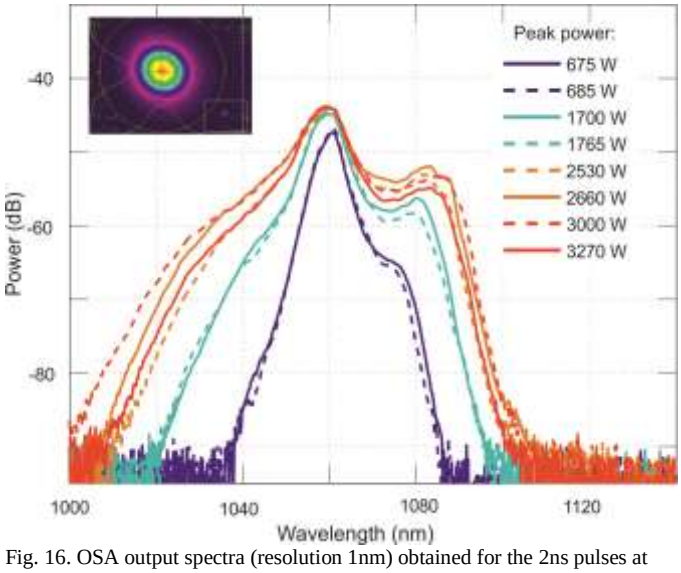

Fig. 16. OSA output spectra (resolution 1nm) obtained for the 2ns pulses at 1MHz repetition rate. Solid line: coil diameter 30cm, dashed line: 15cm. Inset: Output beam at ~1065nm at maximum power.

Further tests using a shorter piece of fiber under test (FUT) showed that for the same peak power, much narrower spectra are obtained, which confirms the existence of the FWM phase matched bands in the FUT. In the experiment employing a ~1m long SRS suppression fiber, the peak power was capped at higher value of ~5kW, whilst SRS wavelengths were filtered out from the spectrum. Additional experiments showed that the FWM process has not degraded the output beam quality and the M^2 remained less than 1.1.

The strategies for mitigation of FWM, which also include careful design of the fiber effective area and dispersion properties, are still ongoing and the results will be presented elsewhere.

We also investigated the high average power handling capability of the SRS suppression fibre by transmitting 800W from a high power single mode fibre laser operating at 1070 nm. The SRS mitigating fibre was spliced at both end with a single mode matched passive ensuring single mode excitation and single mode transmission.

VII. CONCLUSION

We have reported on a novel fiber for the filtering of stimulated Raman scattering for high average or high peak optical power delivery applications. The fiber is based on the series of circularly arranged high index Ge rods embedded in a fluorine doped silica cladding. The functionality of the fiber is based on the combination of the wavelength dependent mode delocalization and spatially dependent loss mechanism due to leakage. The key advantage of this novel design is in a significantly reduced sensitivity to bending in comparison to the W-type ring fibers and photonic bandgap fibers counterparts. In particular, the bending radius as small as ~5cm leads to the additional losses in SRS band, whilst keeping low losses at the signal wavelength. The proposed fiber is fabricated using stack-and-draw technique. The experimental characterization showed the loss extinction in the excess of 20dB at the Raman wavelength band.

The fiber was used experimentally as a 9.5m delivery fiber for the 2ns pulses laser and showed a good output beam

quality at the peak powers of up to ~3kW. Importantly, preliminary results open up the potential for the new class of SRS filtering fiber to find use in high power fiber laser applications. Further investigation will focus on the means to mitigate the four-wave mixing, and to explore designs that would be even easier to fabricate. The observed propagation loss saturation effect at the SRS band with fiber length can potentially limit the deployment of such SRS filtering fibers in high power laser systems. We are currently investigating alternative designs that can overcome this effect.

REFERENCES

[1] M. N. Zervas, and C. A. Codemard, (2014, April). High power fiber lasers: a review, *IEEE J. of Sel. Topics in Quantum Electronics 20(5)*, pp. 0904123.

[2] C. Jauregui, J. Limpert, and A. Tünnermann, (2013, Oct.). High-power fiber lasers, *Nat. Photonics 7*, pp. 861-867.

[3] T. T. Alkeskjold, (2009, Sep.). Large-mode-area Ytterbium-doped fiber amplifier with distributed narrow spectral filtering and reduced bend sensitivity, *Opt. Exp. (19)*, pp. 16394-16405.

[4] T. T. Alkeskjold, (2010, July.). Single-mode large-mode area fiber amplifier with higher-order mode suppression and distributed passband filtering of ASE and SRS, *Proc. of SPIE Photonic West 7580*, pp. 758012-1

[5] R. H. Stolen, E. P. Ippen, and A. R. Tynes, (1972, Aug.). Raman oscillations in glass optical waveguide, *Appl. Phys. Lett. 20(62)*, pp. 62-64.

[6] M. N. Zervas, "Power scalability in high power fiber amplifiers," CLEO Europe, paper cj-6-1 (2017).

[7] D. Nodop, C. Jauregui, F. Jansen, J. Limpert, and A. Tünnermann, (2010, Sep.). Suppression of stimulated Raman scattering employing long period gratings in double-clad fiber amplifiers, *Opt. Lett. 35(17)*, pp. 2982-2984.

[8] J. Kim, C. Dupriez, C. Codemard, J. Nilsson, and J. K. Sahu, (2006, May). Suppression of stimulated Raman scattering in a high power Yb-doped fiber amplifier using a W-type core with fundamental mode cut-off, *Opt. Exp. 14(12)*, pp. 5103-5113.

[9] J. M. Fini, R. T. Bise, M. F. Yan, A. D. Yablon, and P. W. Wisk, (2005, Dec.). Distributed fiber filter based on index-matched coupling between core and cladding, *Opt. Exp. 13(25)*, pp. 10022-10033.

[10] J. M. Fini, M. D. Mermelstein, M. F. Yan, R. T. Bise, P. W. Wisk, and M. J. Andrejco, (2006, Sep.). Distributed suppression of stimulated Raman scattering in an Yb-doped filter-fiber amplifier, *Opt. Lett. 31(17)*, pp. 2550-2552.

[11] V. I. Neves, and A. S. C. Fernandes, (1999, Aug.). Modal characteristics for W-type and M-type dielectric profile fibers, *Micro&Opt. Tech. Lett.*, 22, 2014, pp. 398-405.

[12] H. Wei, P. Yan, S. Chen, W. Tong, J. Luo, and S. Ruan, (2010, May). A broadband ultra-low loss all-solid photonic bandgap fiber, *OFC Conference*, pp. 877-879.

[13] M. Kashiwagi, K. Saitoh, K. Takenaga, S. Tanigawa, S. Matsuo, and M. Fujimaki, (2012, June). Effectively single-mode all-solid photonic bandgap fiber with large effective area and low bending loss for compact high-power all-fiber lasers, *Opt. Exp. 20(14)*, pp. 15061-15070.

[14] B. Ward, (2011, June). Solid-core photonic bandgap fibers for cladding-pumped Raman amplification. *Opt. Exp. 19(12)*, pp. 11852-11866.

[15] F. Gerome, J. L. Auguste, and J. M. Blondy, (2004, June). Design of dispersion-compensating fibers based on a dual-concentric-core photonic crystal fiber. *Opt. Lett. 29(23)*, pp. 2725-2727.

[16] E. A. Kuzin, G. Beltran-Perez, M. A. Basurto_Pensado, R. Rojas-Laguna, J. A. Andrade-Lucio, M. Torres-Cisneros, and E. Alvarado-Mendez, (1999, Oct.). Stimulated Raman scattering in a fiber with bending loss. *Opt. Comm. 169*, pp. 87-91.

[17] P. D. Dragic, (2005, Feb.). Suppression of first order stimulated Raman scattering in Erbium-doped fiber laser based LIDAR transmitters through induced bending loss. *Opt. Comm. 250*, pp. 403-410.

[18] N. Vukovic, J. S. Chan, P. M. Gorman, M. N. Petrovich, J. R. Hayes, A. Malinowski, C. A. Codemard, and M. N. Zervas, (2017, Jan.). Design and characterisation of SRS filtering optical fiber for pulsed fiber laser beam delivery. *Proc. of SPIE Photonic West* 10083, pp. 1008312-1.

[19] E. M. Dianov, (1994). Fluorine-doped silica optical fibres fabricated using plasma-chemical technologies. *Proc. SPIE 2425*, pp. 53-57.

Dr Christophe A. Codemard graduated from École Nationale Supérieure Des Sciences Appliquées et de Technologie, Lannion, France, in optoelectronics in 1999 and obtained his Ph.D. degree from the Optoelectronics Research Centre, Southampton University, U.K., in 2007.
He is currently Advanced Research Manager at SPI Lasers and leads the Advanced Laser Laboratory. His main research interests include high power rare-earth doped fiber lasers and amplifiers, pulsed fiber lasers, nonlinear effects and numerical simulations. He has published more than 150 papers in scientific journals and conference proceedings.

Dr Natasha T. Vukovic received her B.Sc., M.Sc., and Ph.D. degrees in electronics from the Faculty of Electronics Engineering, University of Nis, Nis, Serbia, and the Ph.D. degree in photonics from the Optoelectronics Research Centre, Southampton, U.K. She joined the Optoelectronics Research Centre, Southampton, in 2010. She is currently Senior Research Fellow with the Advanced Laser Laboratory. Her main research interests include specialty fiber design for fiber lasers, nonlinear fiber optics, and tapered optical fibers.

Dr Jaclyn Chan, biography not available at the time of publication.

Dr Paulo J. Almeida received the degree in Physics and Applied Mathematics from the University of Porto, Porto, Portugal; the M.Sc. degree in Electronics and Computer Science from the Technical University of Lisbon, Lisbon, Portugal; and the Ph.D. degree in Optoelectronics from the Optoelectronics Research Centre (ORC) at the University of Southampton, Southampton, U.K in 2006. He was a postdoctoral research fellow with the Pulsed Fibre Laser group at the ORC between 2006 and 2007, and joined Fianium Ltd. in 2007 has a senior development Engineer where he worked in the development of mode-locked picosecond and femtosecond fibre lasers until 2017. He is currently a Principal Fibre Laser Engineer at SPI Lasers Ltd. His current research interests include ultrafast fibre lasers, mode-locked lasers, high-power pulsed fibre lasers.

Dr John R. Hayes, biography not available at the time of publication.

Dr Marco N. Petrovich, biography not available at the time of publication.

Dr Catherine Baskiotis, biography not available at the time of publication.

Dr Andrew Malinowski received a BA in Natural Sciences from the University of Cambridge in 1992 and a PhD in Physics from the University of Southampton in 1996. He has worked at the University of Sheffield (1996-97) and the University of Southampton (1997-2011). Since 2011 he has been with SPI Lasers, Southampton, UK, working on fiber laser development.

Professor Michalis N. Zervas holds a Royal Academy of Engineering Chair in Advanced Fibre Laser Technologies for Future Manufacturing. His research activities include advanced optical fibre amplifier configurations, high power fibre lasers, fibre DFB lasers, Bragg grating theory and devices, surface-plasmon effects and devices, optical microresonators, and non-linear fibre optics. He is a co-founder of Southampton Photonics Inc., a University of Southampton spin-off, now SPI Lasers Ltd, manufacturing high power fibre lasers, where he served as Chief Scientist from 2003 to 2016. He has authored/coauthored over 320 technical publications, about 45 patents/patent applications (of which 20 are granted) and has served on various conference program committees. He has given a number of invited talks, tutorials and short courses in fiber amplifiers, fibre lasers and fiber Bragg gratings at major international conferences. He was a guest editor of the journal "Journal of Selected Topics in Quantum Electronics", special issue on Advanced Fibres and Waveguides. In 1996 he was awarded the Metrology award from the Confederation of British Industry for his work on fiber Bragg grating characterisation. In 2006 he was finalist for the Royal Society of Engineering McRobert Award for the development of high power industrial fibre lasers. He is Associate Editor of Optics Express and an Optical Society of America Fellow since 2015.